Multiple Hypothesis Data Association for Multipath-Assisted Positioning

Markus Ulmschneider, Christian Gentner, Thomas Jost and Armin Dammann
German Aerospace Center (DLR), Institute of Communications and Navigation, 82234 Wessling, Germany
{markus.ulmschneider,christian.gentner,thomas.jost,armin.dammann}@dlr.de

***Abstract*—Global navigation satellite system denied scenarios such as urban canyons or indoors cause a need for alternative precise localization systems. Our approach uses terrestrial signals of opportunity in a multipath-assisted positioning scheme. In multipath-assisted positioning, each multipath component arriving at a receiver is treated as a line-of-sight signal from a virtual transmitter. While the locations of the virtual transmitters are unknown, they can be estimated simultaneously to the user position using a simultaneous localization and mapping (SLAM) approach. An essential feature of SLAM is data association. This paper addresses the data association problem in multipath-assisted positioning, i.e., the identification of correspondences among physical or virtual transmitters. If a user recognizes a previously observed transmitter, it can correct its own position estimate. We generalize a previous version of our multiple hypothesis tracking scheme for data association in multipath-assisted positioning and show by means of simulations how data association improves the positioning accuracy.**

***Index Terms*—Channel-SLAM, data association, multipath-assisted positioning, simultaneous localization and mapping**

I. Introduction

The vision of autonomous cars is driving a lot of research efforts on precise positioning of road users. Though, the knowledge of a road user's location is a requirement not only for autonomous cars, but for a huge number of conceivable services. The accuracy of global navigation satellite systems (GNSSs) is often sufficient for classical navigation applications when a clear open sky condition is met. However, urban canyons, tunnels or parking garages are examples for scenarios where positioning using GNSS might show a drastically decreased performance or even fail completely due to signal blocking or multipath propagation, for example.

In contrast, various terrestrial based radio frequency (RF) signals of opportunity (SoOs) offer high coverage, often with a high received signal strength. In particular, cellular networks are available in virtually every urban area. Though, multipath propagation affects also terrestrial signals. Especially in GNSS denied areas such as in urban canyons or indoors, a high multipath propagation can be expected causing a bias in range estimates using standard correlator based methods. Standard approaches to mitigate multipath effects at the receiver include the estimation of the channel impulse response (CIR) and the removal of the influence of multipath components (MPCs) on the line-of-sight (LoS) path. However, MPCs themselves contain information on the position of a user, which can be exploited in a multipath-assisted positioning approach.

Multipath-assisted positioning schemes have been proposed for example for radar or indoor ultra-wideband (UWB) systems in [1] and [2], respectively. In both cases, the environment and hence the location of physical and virtual transmitters is assumed to be known. The authors of [3] have presented an algorithm called Channel-SLAM where no such prior information is required. Each MPC of a terrestrial SoO is regarded as being sent by a virtual transmitter in a pure LoS condition to the user. In a general setting, the locations of both the physical and the virtual transmitters are unknown, but can be estimated in addition to the user position. This problem has the structure of a simultaneous localization and mapping (SLAM) problem [4], where the user position and the locations of landmarks are estimated simultaneously. In Channel-SLAM, landmarks correspond to transmitters.

A critical part in SLAM is data association, which is to identify correspondences among landmarks as the user travels through a scenario. In multipath-assisted positioning, we can regard this problem as to find which signal components, or transmitters, correspond. Data association is also of importance when several users travel through the same scenario. Then, information about physical and virtual transmitters can be exchanged among users, for example using local dynamic maps (LDMs) in an intelligent transportation system (ITS) context. Correspondences among the transmitters in such a map and transmitters observed by the user need to be found.

In [5], we presented a first solution to the data association problem in Channel-SLAM based on a method introduced in [6] with the constraint that no more than one transmitter is initialized at each time instant. Within this paper, we present an extension to the results of [5] to overcome this constraint, and discuss data association when users exchange maps.

This paper is structured as follows: In Section II, we derive the Channel-SLAM algorithm in its current state. We present the data association method for Channel-SLAM from [5] and extend it in Section III. Evaluations based on simulations in an urban scenario are presented in Section IV. Finally, Section V concludes the paper.

II. Multipath-Assisted Positioning

A. Virtual Transmitters

The idea of multipath-assisted positioning is to regard every MPC arriving at the receiver as a signal from a virtual

978-1-5386-3089-1/17/$31.00 ©2017 IEEE

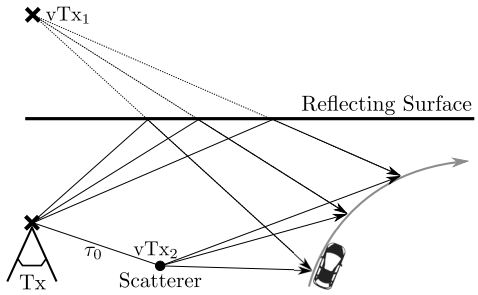

Fig. 1. The signal from the physical transmitter Tx is received by a mobile user via two different propagation paths. The user considers the received MPC reflected by the surface as being transmitted by the virtual transmitter vTx_1, and the MPC scattered at the punctual scatterer as being transmitted by the virtual transmitter vTx_2.

transmitter in a pure LoS condition as illustrated in Fig. 1. A user receives the signal from the physical transmitter Tx via two different propagation paths. The MPC reflected at the surface is interpreted as a LoS signal from the virtual transmitter vTx_1, which is located at the apparent origin of the signal. While the reflection point moves along the wall as the user moves, the location of vTx_1 is static, and it is the location of the physical transmitter mirrored at the reflecting surface. Furthermore, the virtual and the physical transmitter are inherently perfectly time synchronized.

Likewise, the MPC scattered at the punctual scatterer is regarded as being transmitted by the virtual transmitter vTx_2, which is located at the scatterer's position. For scattering, we assume the energy of the electromagnetic wave impinging against a punctual scatterer to be emitted uniformly in all directions. Though, in the case of scattering, the physical and the virtual transmitter are not time synchronized: there is a delay offset τ_0 among the two, which is the actual propagation distance of the signal from the physical to the virtual transmitter divided by the speed of light. This delay offset can be interpreted as a clock offset. The concept of an RF signal being reflected or scattered once can be generalized to the case where a signal is reflected or scattered multiple times by simple geometrical considerations [3].

B. Channel-SLAM

The propagation channel is assumed to be a linear and time-variant multipath channel. Hence, the CIR is modeled as a superposition of signal components with a certain time of arrival (ToA), complex amplitude, and angle of arrival (AoA). Fig. 2 summarizes the Channel-SLAM algorithm briefly. Given the received signal, the parameters of the signal components arriving at the receiver are estimated. Based on these estimates, the states of the physical and virtual transmitters and the user state are estimated simultaneously in a SLAM approach. Additional sensor data, such as from an inertial measurement unit (IMU), can be incorporated in the estimation process. As Channel-SLAM does not differentiate between physical and virtual transmitters, the term transmitter is used generally to refer to any of the two in the following.

For the estimation of the signal parameters in the first step of Channel-SLAM, we use the Kalman enhanced super resolution

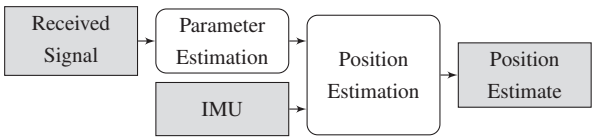

Fig. 2. Overview on the two steps of the Channel-SLAM algorithm.

tracking (KEST) algorithm [7]. KEST estimates parameters of the received signal components and tracks them over time with a Kalman filter. In addition, it keeps track of the number of signal components. Signal parameters can be the amplitude, phase, ToA or AoA, depending on the available hardware and the scenario. For Channel-SLAM, the ToAs and AoAs of the signal components are of interest. The super resolution method in KEST is necessary as we use a signal with a bandwidth of $100\,\mathrm{MHz}$ at a center frequency of $1.5\,\mathrm{GHz}$ in the simulations. The single signal components are assumed independent from each other, i.e., we assume they interact with distinct objects.

At each time instant k, we stack the corresponding KEST estimates for the detected signal components in the vector $\boldsymbol{z}_k$,

$$\boldsymbol{z}_k = \left[\boldsymbol{d}_k^T \;\; \boldsymbol{\theta}_k^T\right]^T, \tag{1}$$

where $\boldsymbol{d}_k$ are the ToA estimates of the N_{TX} signal components,

$$\boldsymbol{d}_k = \left[d_{1,k} \;\ldots\; d_{N_{\mathrm{TX}},k}\right]^T, \tag{2}$$

and $\boldsymbol{\theta}_k$ are the corresponding N_{TX} AoA estimates,

$$\boldsymbol{\theta}_k = \left[\theta_{1,k} \;\ldots\; \theta_{N_{\mathrm{TX}},k}\right]^T. \tag{3}$$

Note that each signal component corresponds to one transmitter. When the number of detected signal components changes over time, the number of transmitters changes as well. In particular, when KEST detects a new signal component, a new transmitter is initialized based on the estimate. Likewise, when KEST loses track of a signal component, the corresponding transmitter is discarded. Nevertheless, for notational convenience, we drop the time instant index k in N_{TX}.

For the second step in Channel-SLAM, we simultaneously estimate the state of the transmitters and the state of the user. The user state vector at time instant k is defined as

$$\boldsymbol{x}_{\mathrm{u},k} = \left[x_k \;\; y_k \;\; v_{x,k} \;\; v_{y,k}\right]^T, \tag{4}$$

consisting of the user position and velocity in two dimensions. The state vector of the j^{th} transmitter contains its location in two dimensions and its clock offset $\tau_{0,k}^{<j>}$, namely

$$\boldsymbol{x}_{\mathrm{TX},k}^{<j>} = \left[x_{\mathrm{TX},k}^{<j>} \;\; y_{\mathrm{TX},k}^{<j>} \;\; \tau_{0,k}^{<j>}\right]^T. \tag{5}$$

Hence, the combined state vector $\boldsymbol{x}_k$ consisting of the user and the N_{TX} transmitter states is expressed as

$$\begin{aligned}\boldsymbol{x}_k &= \left[{\boldsymbol{x}_{\mathrm{u},k}}^T \;\; {\boldsymbol{x}_{\mathrm{TX},k}}^T\right]^T \\ &= \left[{\boldsymbol{x}_{\mathrm{u},k}}^T \;\; {\boldsymbol{x}_{\mathrm{TX},k}^{<1>}}^T \;\ldots\; {\boldsymbol{x}_{\mathrm{TX},k}^{<N_{\mathrm{TX}}>}}^T\right]^T.\end{aligned} \tag{6}$$

The overall goal is to find the posterior probability density function (PDF) of the state vector $\boldsymbol{x}_{0:k}$ at all time instants up to k given the available measurements $\boldsymbol{z}_{1:k}$ from Eq. (1), i.e., $\mathrm{p}\left(\boldsymbol{x}_{0:k}|\boldsymbol{z}_{1:k}\right)$. We can factorize the posterior PDF into a

product of the user and the transmitters state posterior PDFs, namely

$$\begin{aligned}\mathrm{p}\left(\boldsymbol{x}_{0:k}|\boldsymbol{z}_{1:k}\right) &= \mathrm{p}\left(\boldsymbol{x}_{\mathrm{TX},0:k}, \boldsymbol{x}_{\mathrm{u},0:k}|\boldsymbol{z}_{1:k}\right) \\ &= \mathrm{p}\left(\boldsymbol{x}_{\mathrm{u},0:k}|\boldsymbol{z}_{1:k}\right)\mathrm{p}\left(\boldsymbol{x}_{\mathrm{TX},0:k}|\boldsymbol{z}_{1:k}, \boldsymbol{x}_{\mathrm{u},0:k}\right). \quad (7)\end{aligned}$$

With the assumption of signal components and hence the transmitters being independent from each other, we can further factorize the conditioned transmitters posterior PDF to

$$\mathrm{p}\left(\boldsymbol{x}_{\mathrm{TX},0:k}|\boldsymbol{z}_{1:k}, \boldsymbol{x}_{\mathrm{u},0:k}\right) = \prod_{j=1}^{N_{\mathrm{TX}}} \mathrm{p}\left(\boldsymbol{x}_{\mathrm{TX},0:k}^{<j>}|\boldsymbol{z}_{1:k}^{<j>}, \boldsymbol{x}_{\mathrm{u},0:k}\right), \quad (8)$$

where $\boldsymbol{z}_{1:k}^{<j>} = \left[d_{j,1:k} \;\; \theta_{j,1:k}\right]^T$ is the measurement for the j^{th} transmitter.

We use Bayesian recursive estimation to actually estimate the PDF in Eq. (7). In general, Bayesian recursive estimation schemes work in two steps. In the prediction step, the state estimate for the next time step is predicted based on a movement model. In the update step, the state estimate is updated based on the measurements.

As we consider a static scenario, where the locations of physical transmitters and objects reflecting and scattering the RF signals do not change, the locations of virtual transmitters are static as well. Hence, in the prediction step for the j^{th} transmitter, we define the transition prior as

$$\mathrm{p}\left(\boldsymbol{x}_{\mathrm{TX},k}^{<j>}|\boldsymbol{x}_{\mathrm{TX},k-1}^{<j>}\right) = \delta\left(\boldsymbol{x}_{\mathrm{TX},k}^{<j>} - \boldsymbol{x}_{\mathrm{TX},k-1}^{<j>}\right). \quad (9)$$

For the transition prior for the user, we assume to have heading change rates, or yaw rates, from a gyroscope available at the user. However, we do not assume to have any additional knowledge on the users movement, and the user speed is modeled by a random walk model. A detailed description of the user transition prior is given in [3], [8].

In the update step in Bayesian recursive estimation, we incorporate the estimates from Eq. (1) as measurements. The measurement noise is assumed to be zero-mean Gaussian distributed for both the ToA and the AoA measurements with variances $\sigma_{d,j}^2$ and $\sigma_{\theta,j}^2$, respectively. The likelihood for the measurements can then be expressed as

$$\mathrm{p}\left(\boldsymbol{z}_k|\boldsymbol{x}_k\right) = \prod_{j=1}^{N_{\mathrm{TX}}} \mathcal{N}\left(d_{j,k}; \hat{d}_{j,k}, \sigma_{d,j}^2\right)\mathcal{N}\left(\theta_{j,k}; \hat{\theta}_{j,k}, \sigma_{\theta,j}^2\right), \quad (10)$$

where $\mathcal{N}\left(x; \mu, \sigma^2\right)$ denotes a Gaussian PDF in x with mean μ and variance σ^2, and the predicted ToA and AoA for the j^{th} transmitter are

$$\hat{d}_{j,k} = \frac{1}{c_0}\sqrt{(x_k - x_{\mathrm{TX},k}^{<j>})^2 + (y_k - y_{\mathrm{TX},k}^{<j>})^2} + \tau_{0,k}^{<j>}, \quad (11)$$

where c_0 denotes the speed of light, and

$$\hat{\theta}_{j,k} = \mathrm{atan2}\left(y_k - y_{\mathrm{TX},k}^{<j>}, x_k - x_{\mathrm{TX},k}^{<j>}\right) - \mathrm{atan2}\left(v_{y,k}, v_{x,k}\right), \quad (12)$$

respectively. The function $\mathrm{atan2}\left(y, x\right)$ defines the four quadrant inverse tangent function. In the two-dimensional Cartesian coordinate system, it returns the counter-clockwise angle between the positive x-axis and the point given by the coordinates (x, y).

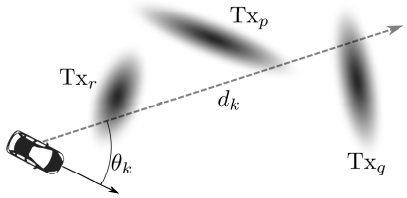

Fig. 3. The KEST algorithm detects a new signal component with ToA d_k and AoA θ_k. It might correspond to any of the old transmitters Tx$_p$,Tx$_q$, and Tx$_r$, or to a new transmitter. The current state estimates of the old transmitters are represented by the ellipses.

Because of the nonlinearities in Eq. (11) and in Eq. (12), we use a Monte Carlo method, namely a Rao-Blackwellized particle filter [3], [4] to solve the Bayesian recursive estimation problem. The user state posterior PDF is represented by a number of N_p particles. The i^{th} user particle is denoted by $\boldsymbol{x}_{\mathrm{u},k}^{<i>}$ and has an associated weight $w_k^{<i>}$. The user state PDF is approximated by

$$\mathrm{p}\left(\boldsymbol{x}_{\mathrm{u},k}|\boldsymbol{z}_{1:k}\right) = \sum_{i=1}^{N_p} w_k^{<i>}\delta\left(\boldsymbol{x}_{\mathrm{u},k} - \boldsymbol{x}_{\mathrm{u},k}^{<i>}\right). \quad (13)$$

Due to the structure of the factorization in Eq. (7) and in Eq. (8), each user particle has N_{TX} particle filters associated to itself, that estimate the states of the N_{TX} transmitters. The state posterior PDF for the j^{th} transmitter of the i^{th} user particle is approximated by

$$\mathrm{p}\left(\boldsymbol{x}_{\mathrm{TX},k}^{<i,j>}|\boldsymbol{z}_{1:k}, \boldsymbol{x}_{\mathrm{u},k}^{<i>}\right) = \sum_{l=1}^{N_{p,\mathrm{Tx}}} w_k^{<i,j,l>}\delta\left(\boldsymbol{x}_{\mathrm{TX},k}^{<i,j>} - \boldsymbol{x}_{\mathrm{TX},k}^{<i,j,l>}\right), \quad (14)$$

where $N_{p,\mathrm{Tx}}$ is the number of particles representing one transmitter, $\boldsymbol{x}_{\mathrm{TX},k}^{<i,j,l>}$ is the l^{th} particle of the j^{th} transmitter for the i^{th} user particle, and $w_k^{<i,j,l>}$ its associated weight. Note that the number of particles may be different for different transmitters of different user particles. Though, we drop the user particle and transmitter indices in $N_{p,\mathrm{Tx}}$ for notational convenience. For an actual implementation of the Rao-Blackwellized particle filter including the particle weight updates, we refer to [3].

III. Data Association

As the user travels through a scenario, the KEST estimator may lose and regain track of a signal component corresponding to a propagation path, and thus, the user loses and regains track of the corresponding transmitter. We define the set of transmitters that have been observed earlier, but are not observed at the current time instant, as *old* transmitters. Every time KEST detects a new signal component, a new transmitter is initialized, and there are two possible cases:

1) the new transmitter is indeed a new transmitter that had never been observed before, or
2) the new transmitter corresponds to an old transmitter that had been observed before.

The association problem we face is essentially the question for which case to decide, and, in the second case, to which

old transmitter the new one corresponds.

Fig. 3 illustrates an example for the association problem, showing the posterior PDFs of the three old transmitters Tx_p, Tx_q and Tx_r. A new signal component is detected by KEST with ToA d_k and AoA θ_k. The question is if the signal component corresponds to any of the three old transmitters, or to a new one. Note that due to a possible delay offset of the transmitters as in Eq. (5), each of the associations might be more or less likely.

With correct associations among transmitters, the user state estimate can be corrected at least to a certain extent. Hence, data association is essential for the robustness of long-term SLAM. Though, data association is an underdetermined problem in our case, since the measurement for a transmitter at one time step is of less dimensions than the state of a transmitter. To be able to remove wrong associations at later time instants, we employ a multiple hypothesis tracking (MHT) tracking scheme. Every user particle decides for associations among new and old transmitters on its own. The weights of particles that have decided for wrong associations are likely to decrease over time, and these particles are likely not to be resampled in the resampling step of the particle filter.

In the following, we describe how to decide for associations for one user particle i. For notational convenience, we omit the index i from here on in the variables related to associations.

A. Initialization of One Transmitter

Within this subsection, we summarize the results from [5] where we consider the case where there is at most one new transmitter to be initialized per time instant, i.e., where KEST detects at most one new signal component.

The set Υ_k contains the indices of transmitters that may be associated with the new transmitter at time instant k. These are old transmitter that have not yet been associated with any other transmitter. The association variable n_k denotes the index of the old transmitter that the new transmitter is associated with.

We denote the marginalized likelihood of the measurement $\boldsymbol{z}_k$ at time instant k for user particle i by p_{n_k}, assuming an association of a new transmitter with the old transmitter n_k. It is defined as [6]

$$p_{n_k} = \psi_c\left(n_k, \Upsilon_k\right) \mathrm{p}\left(\boldsymbol{z}_k | n_k, N_{k-1}, \boldsymbol{x}_{\mathrm{u},k}^{<i>}, \boldsymbol{z}_{1:k-1}\right), \quad (15)$$

where N_{k-1} is a set of tuples describing association decisions up to time instant $k-1$. The function

$$\psi_c\left(n_k, \Upsilon_k\right) = \begin{cases} 1 & \text{if } n_k \in \Upsilon_k \\ 0 & \text{else} \end{cases} \quad (16)$$

is a consistency function ensuring that the new transmitter can be associated only with old transmitters that have not yet been associated.

Following [5], where we use the structure of the Rao-Blackwellized particle filter and Eq. (14), the marginalized likelihood p_{n_k} is

$$\begin{aligned} p_{n_k} =& \psi_c\left(n_k, \Upsilon_k\right) \\ & \times \sum_{l=1}^{N_{p,\mathrm{Tx}}} w_k^{<i,n_k,l>} \mathrm{p}\left(\boldsymbol{z}_k | \boldsymbol{x}_{\mathrm{TX},k}^{<i,n_k,l>}, n_k, N_{k-1}, \boldsymbol{x}_{\mathrm{u},k}^{<i>}\right), \end{aligned} \quad (17)$$

where $\boldsymbol{x}_{\mathrm{TX},k}^{<i,j,l>}$ is the l^{th} particle of the j^{th} transmitter of the i^{th} user particle, and $w_k^{<i,j,l>}$ its associated weight.

To reduce the computational complexity, we regard only those old transmitters from Υ_k for associations whose likelihood for the new measurement exceeds a threshold ρ. We denote a set of indices of these transmitters by Γ_k,

$$\Gamma_k = \{j : j \in \Upsilon_k \wedge p_j > \rho\}. \quad (18)$$

Two strategies for actually choosing an association are considered in the following, namely a maximum likelihood (ML) method and data association sampling (DAS) [5], [6]. The ML method decides for the association of the new transmitter with the old transmitter $\hat{n}_{\mathrm{ML},k}$ by

$$\hat{n}_{\mathrm{ML},k} = \underset{n_k \in \Gamma_k \cup \{0\}}{\arg\max}\ p_{n_k}, \quad (19)$$

where p_0 is defined to be the probability for deciding for no association. For DAS, we sample an association of the new transmitter with the old transmitter $\hat{n}_{\mathrm{DAS},k}$ randomly based on the likelihoods cp_{n_k} for $n_k \in \Gamma_k \cup \{0\}$, where c denotes a normalization constant. Note again that for $\hat{n}_k = 0$, we choose not to make an association for the new transmitter. If $\hat{n}_k > 0$, the tuple of the new transmitter index and $\hat{n}_k$ is added to N_k.

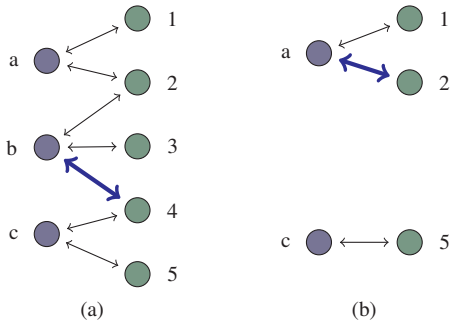

Fig. 4. The purple nodes on the left side of the bipartite graphs represent transmitters that are to be initialized, and the green nodes on the right represent old transmitters. The edges represent possible associations. An association decision among transmitters b and 4 is made in (a), where the blue thick arrow shows the association. Following Algorithm 1, the remaining subgraphs after removing nodes b and 4 from the graph in (a) are depicted in (b). In the upper subgraph, an association decision among transmitters a and 2 is made.

B. Initialization of Multiple Transmitters

Within this subsection, we expand the results from Subsection III-A to the case where multiple new transmitters are initialized at the same time instant. Again, each particle takes its own decision on associations. We apply a greedy algorithm to decide for associations. We explain this algorithm exemplarily by Fig. 4, where we have three new transmitters a, b and c to be initialized, and five old transmitters 1, 2,

3, 4 and 5 that may be associated. We denote the set of new transmitters by $\mathcal{M}_k$ and hence have $\Upsilon_k = \{1, 2, 3, 4, 5\}$, and $\mathcal{M}_k = \{a, b, c\}$. The new transmitters from $\mathcal{M}_k$ are represented in the bipartite graph in Fig. 4(a) by the purple nodes on the left side, while the old transmitters from Υ_k are represented by green nodes on the right side.

The association tuple (n_k, m) denotes the association among the old transmitter $n_k \in \Upsilon_k$ and the new transmitter $m \in \mathcal{M}_k$. For each possible association (n_k, m), we calculate the marginalized likelihood $p_{n_k,m}$ of the measurement $\boldsymbol{z}_k^{<m>}$ for the new transmitter m similar to Eq. (17), namely

$$p_{n_k,m} = \psi_c\left(n_k, \Upsilon_k\right) \sum_{l=1}^{N_{p,\mathrm{Tx}}} w_k^{<i,n_k,l>} \times \mathrm{p}\left(\boldsymbol{z}_k^{<m>} | \boldsymbol{x}_{\mathrm{TX},k}^{<i,n_k,l>}, (n_k, m), N_{k-1}, \boldsymbol{x}_{\mathrm{u},k}^{<i>}\right). \tag{20}$$

To reduce the computational complexity, we regard only those associations for which the likelihood $p_{n_k,m}$ exceeds a threshold ρ. Therefore, the set of possible associations is the set of tuples

$$\Gamma_k = \{(j, m) : j \in \Upsilon_k \wedge m \in \mathcal{M}_k \wedge p_{j,m} > \rho\}. \tag{21}$$

Each edge among a new and an old transmitter in Fig. 4 represents a possible association, i.e., a tuple from Γ_k. There is no edge representing the decision for no association drawn explicitly. From all possible associations, i.e., edges in Fig. 4(a), we chose one based on the ML method or DAS. For the ML method, we choose the association with highest likelihood,

$$(\hat{n}_k, \hat{m})_{\mathrm{ML}} = \underset{(n_k,m)\in\Gamma_k\cup\{(0,0)\}}{\arg\max} p_{n_k,m}, \tag{22}$$

where $p_{0,0}$ denotes the likelihood for no association. For DAS, an association $(\hat{n}_k, \hat{m})_{\mathrm{DAS}}$ is sampled randomly from the likelihoods $cp_{n_k,m}$ for $(n_k, m) \in \Gamma_k \cup \{(0, 0)\}$, where c is a normalization constant.

In the case that no association has been chosen, we are done. Otherwise, we remove the two nodes $\hat{n}_k$ and $\hat{m}$ that have been associated from the graph. In Fig. 4(a), for example, the thick blue arrow indicates an association of the new transmitter $\hat{m} = b$ with the old transmitter $\hat{n}_k = 4$. Thus, after removing the two nodes, two bipartite subgraphs are left as shown in Fig. 4(b). We repeat the above steps for the two remaining graphs, deciding for an association among transmitters a and 2 in the upper subgraph, again indicated by the thick blue arrow. In the lower subgraph, we decide for no association in this example, and hence transmitters c and 5 are not associated. Algorithm 1 sums up the single steps for one time instant in the general case.

Algorithm 1: Greedy Algorithm for Initializing Multiple Transmitters with Data Association

```
Data: new transmitters M_k and old transmitters Υ_k
Result: list of associations
create the set Γ_k as in Eq. (24);
create the bipartite graph as in Fig. 4;
if there are possible associations then
    decide for one association (ML or DAS) among all edges;
    if decision for no association then
        return;
    else
        add association to list of associations;
        remove associated nodes from bipartite graph;
        apply this algorithm on all remaining subgraphs with corresponding subsets of M_k and Υ_k;
else
    return;
```

C. Prior Maps

When multiple users travel through the same scenario, they might exchange maps of transmitters. If prior knowledge in form of such a prior map is available, the above methods may be as well applied to find associations among new transmitters and transmitters from such a map. However, the coordinate systems of the user and the map need to be the same, or their relative offset and rotation need to be known. This is the case if for example the starting positions and directions of users are known. We will regard only the case where no more than one transmitter is initialized at each time instant, since a generalization to the case where multiple transmitters are initialized is straightforward following Subsection III-B.

The set of transmitters in the prior map that have not yet been associated is denoted by $\tilde{\Upsilon}_k$, and $\tilde{n}_k$ denotes the index of the transmitter in the prior map that the new transmitter is associated with. The marginalized likelihoods can be computed similar to Eq. (15) as

$$p_{\tilde{n}_k} = \sum_{l=1}^{N_{p,\mathrm{Tx}}} w_k^{<i,\tilde{n}_k,l>} \mathrm{p}\left(\boldsymbol{z}_k | \boldsymbol{x}_{\mathrm{TX},k}^{<i,\tilde{n}_k,l>}, \tilde{n}_k, N_{k-1}, \boldsymbol{x}_{\mathrm{u},k}^{<i>}\right) \times \psi_c\left(\tilde{n}_k, \tilde{\Upsilon}_k\right). \tag{23}$$

The set Γ_k for the case that both old transmitters estimated by the user so far and transmitters from the prior map can be associated with the new transmitter is similar to Eq. (18),

$$\Gamma_k = \{j : (j \in \Upsilon_k \vee j \in \tilde{\Upsilon}_k) \wedge p_j > \rho\}. \tag{24}$$

IV. Simulations

A top view on the urban simulation scenario with one physical transmitter and a mobile user is depicted and described in Fig. 5. The physical transmitter continuously broadcasts a known signal at a carrier frequency of 1.5 GHz with a bandwidth of 100 MHz. With ray-tracing, the received signal is simulated for every user position. We assume the signal is reflected and/or scattered at most two times on its way from the physical transmitter to the user. The signal-to-noise-ratio (SNR) averaged over all user positions is 7 dB.

The user is equipped with a 2-dimensional antenna array with nine elements. This allows the KEST algorithm to estimate both the ToAs and the AoAs of the signal components at the receiver as in Eq. (1). The update rate of the measurements, or KEST estimates, is 20 Hz.

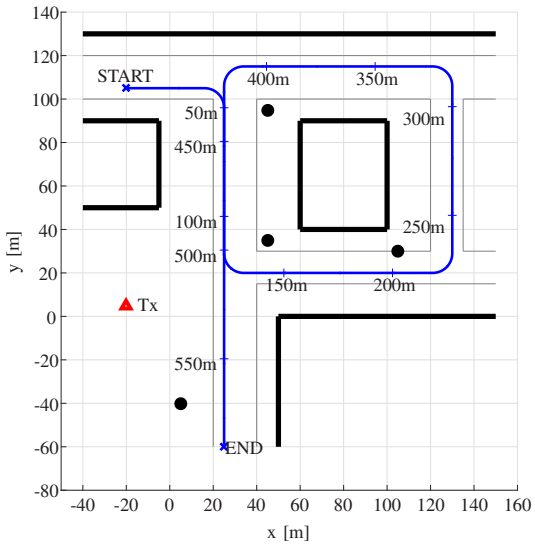

Fig. 5. The user moves through the urban simulation scenario along the blue track from START to END with a constant speed of $10\,\mathrm{m/s}$. The physical transmitter is denoted by the red triangle labeled Tx. Thick black lines are reflecting walls, black dots are scatterers.

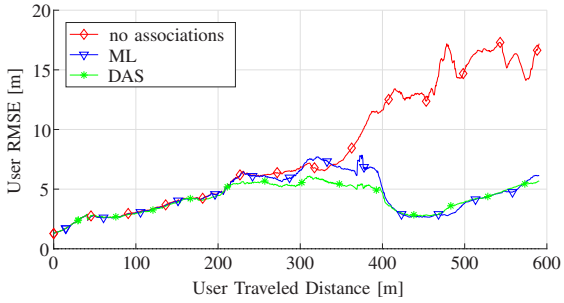

Fig. 6. The user RMSE of the versus the user traveled distance.

In order to define a local coordinate system, we assume the initial position and direction of the user to be known. Thus, for initialization, 3000 user particles are distributed around the true initial position of the user with a variance of $1\,\mathrm{m}^2$. Additionally, an IMU is simulated at the user, from which only heading change rates are used. The speed of the user is modeled by a random walk model. No prior map of transmitters is used here, and no prior information on the states of the transmitters is assumed.

The RMSE for the user position versus its traveled distance averaged over 300 runs is depicted in Fig. 6. The red curve shows the RMSE if no associations among transmitters are made. For the ML method and DAS, the RMSEs are plotted in blue and green, respectively. As mentioned above, the initial state of the user is assumed to be known and hence the RMSE is very low at the initial position. In the case of no associations, the RMSE increases nearly linearly with the traveled distance with some fluctuations. As expected, the red curve coincides with the blue and the green curve during the first approximately $200\,\mathrm{m}$, where no associations can be made. After a traveled distance of $350 - 400\,\mathrm{m}$, the user observes multiple old transmitters that had been observed during the first $150\,\mathrm{m}$ of the run, and the user position estimate can be corrected. Therefore, the RMSE decreases for both association methods. While the DAS method shows a slightly better performance in the region of a traveled distance between $210\,\mathrm{m}$ and $400\,\mathrm{m}$, they show a very similar performance throughout the rest of the track. At the end of the track, the user RMSE for both association methods is in the order of $6\,\mathrm{m}$, and approximately $17\,\mathrm{m}$ if no associations are made.

V. Conclusion and Outlook

Within this paper, we have expanded the Channel-SLAM algorithm by data association using a MHT scheme. We have proposed an algorithm that can handle the association among transmitters if multiple new transmitters are initialized at the same time instant. Beyond, we have incorporated data association for transmitters in a prior map. Our simulations in an urban multipath scenario show that data association can correct the user position estimate and hence decreases the user RMSE drastically. The ML and the DAS method show similar performance.

VI. Acknowledgement

This work was partially supported by the EU project HIGHTS (High precision positioning for cooperative ITS applications) MG-3.5a-2014-636537.

References

[1] P. Setlur, G. Smith, F. Ahmad, and M. Amin, "Target Localization with a Single Sensor via Multipath Exploitation," *IEEE Trans. Aerosp. Electron. Syst.*, vol. 48, no. 3, pp. 1996–2014, Jul. 2012.

[2] P. Meissner and K. B. Witrisal, "Multipath-assisted single-anchor indoor localization in an office environment," in *19th International Conference on Systems, Signals and Image Processing (IWSSIP)*, Apr. 2012, pp. 22–25.

[3] C. Gentner, T. Jost, W. Wang, S. Zhang, A. Dammann, and U.-C. Fiebig, "Multipath Assisted Positioning with Simultaneous Localization and Mapping," *IEEE Trans. Wireless Commun.*, vol. 15, no. 9, pp. 6104–6117, Sep. 2016.

[4] H. Durrant-Whyte and T. Bailey, "Simultaneous localization and mapping: part i," *IEEE Robot. Autom. Mag.*, vol. 13, no. 2, pp. 99–110, June 2006.

[5] M. Ulmschneider, C. Gentner, T. Jost, and A. Dammann, "Association of Transmitters in Multipath-Assisted Positioning," in *IEEE Global Communications Conference: Signal Processing for Communications (Globecom SPC)*, Singapore, Singapore, Dec. 2017.

[6] S. Thrun, M. Montemerlo, D. Koller, B. Wegbreit, J. Nieto, and E. Nebot, "FastSLAM: An Efficient Solution to the Simultaneous Localization And Mapping Problem with Unknown Data Association," *Journal of Machine Learning Research*, vol. 4, no. 3, pp. 380–407, 2004.

[7] T. Jost, W. Wang, U. Fiebig, and F. Perez-Fontan, "Detection and Tracking of Mobile Propagation Channel Paths," *IEEE Trans. Antennas Propag.*, vol. 60, no. 10, pp. 4875–4883, Oct. 2012.

[8] M. Ulmschneider, C. Gentner, R. Raulefs, and M. Walter, "Multipath Assisted Positioning in Vehicular Applications," in *13th Workshop on Positioning, Navigation and Communications (WPNC)*, Oct. 2016.